

# ANTIC: A Code for Calculation of Neutral Transport in Cylindrical Plasmas

S. TAMOR

*Laboratory for Applied Plasma Studies, Science Applications, Inc.,  
La Jolla, California 92037*

Received February 20, 1980; revised May 27, 1980

A scheme for computing the steady state transport of neutral atoms cylindrical plasmas is described. The physical model used represents atoms emerging from charge exchange collisions by an isotropic source of neutrals with energy equal to  $3/2$  times the local ion temperature. The process of charge exchange and impact ionization by electrons and ions are included. The transport can be described by an integral equation for the neutral source density, and this equation approximated by a set of algebraic equations for the zone average source densities. A derivation of the appropriate kernel and a technique for computing it are presented. Comparison of computed results with predictions of other, more exact, codes exhibit quite satisfactory agreement for temperatures as high as 10 keV.

## 1. INTRODUCTION

The transport of neutral atoms often plays a significant role in the particle and energy balance of thermonuclear plasmas. Typically, there is an influx of low energy (a few eV) neutral atoms from the wall which, upon penetrating the plasma, can undergo ionization or charge exchange scattering. The former possibility in effect simply adds cold plasma. Charge exchange events, however, replace the cold neutrals by energetic atoms which have a high probability of leaving the system without further interaction and are hence a potentially serious energy loss mechanism. Proper account of such processes must be included in any plasma simulator code.

In most CTR devices currently under study, and even in some full scale reactor concepts, the characteristic mean free path of a neutral atom is not small compared with plasma dimensions, and under these conditions a simple diffusion theory treatment is not justifiable. It has been pointed out [1] that this problem is essentially identical with that of neutron transport and that neutron codes would be readily adaptable to the present problem. An example of this approach is discussed in the paper of Gilligan *et al.* [2], who used the ANISN code which permits a very detailed treatment of energy and momentum transfer in the scattering process.

Unfortunately such codes are much too slow for plasma simulators. In this application the neutral transport routine is usually by far the most time consuming

part of the code so that there is considerable incentive for development of fast special purpose codes which take advantage of whatever simplification the problem has to offer. Some of the early work in this direction is summarized in the review article by Hogan [3].

The code ANTIC (Algorithm for Neutral Transport in Cylinders) described here is such a special purpose routine which is accurate and fast enough for use as a simulator subroutine at least if the number of zones is not too large. The basic simplifying feature upon which the code is based is that charge exchange is a very soft interaction so that the velocity distribution of the outgoing atoms is characteristic of the local ion temperature and independent of the velocity of the incident atom. This is a good approximation for energies  $< 10$  keV which covers most present CTR applications. A consequence of this approximation is that all information about the neutral distribution function is contained in the neutral source density from which the complete distribution function can be constructed by a quadrature. This means that the dimensionality of the problem is only that of the coordinate space and not of both coordinates and velocities. It is straightforward to obtain an integral equation for the neutral source density which can be approximated by a finite set of algebraic equations and solved by standard methods.

Two other codes have recently been developed which are based upon the same concept. The code by Burrell [4] assumes that all cross sections are independent of the neutral energy and describes the charge exchange collision source by a Maxwell distribution at the local ion temperature. The constant cross section approximation is probably valid for plasma temperatures up to a few keV. While this approximation is, strictly speaking, not essential, proper inclusion of the energy dependence would significantly complicate an already elaborate calculation of the integral equation kernel.

The SPUDNUT code of Audenaerde *et al.* [5] keeps the velocity dependence of the cross sections but approximates the distribution function for the newly born neutrals in each zone by an isotropic monoenergetic distribution at energy equal to  $3/2$  times the local plasma temperature. This is an enormous simplification which, in slab geometry, makes calculations of the kernel almost trivial. The restriction to slab geometry, however, limits the applicability of the code to very large systems where the only primary source of neutrals is at the outer walls and there are no significant sources in the interior.

The code described in the present paper is essentially a generalization of SPUDNUT to a cylinder and makes the same spherical shell approximation for the velocity distribution of newly created neutrals. In view of the relatively weak energy dependence of the relevant cross sections this model appears intuitively reasonable, but is not easily justified a priori. It will be shown by comparison of test problems with more exact codes that the code produces quite satisfactory results over the parameter range of interest in most CTR applications.

The next section of this paper is devoted to a discussion of the physical model and its formulation in terms of an integral equation for the neutral source density. In Section 3 we describe the numerical method for approximating the kernel of the

integral equation and the other quantities required to describe the cold influx, escape to the walls, etc. A sampling of numerical results which compares the results of ANTIC with other published results is presented in Section 4. In Appendix A we present a derivation of the integral equation for the neutral source density from the Boltzmann equation, while Appendix B contains a derivation of the discrete zone approximations to the kernel.

## 2. FORMULATION OF THE PROBLEM

Consider a cylindrical plasma column in which the electron and ion temperature and density profiles are known functions of radius. Low energy neutral hydrogen atoms are injected from the wall at a specified rate and energy. It will be assumed that the wall neutrals emerge with a cosine distribution relative to the boundary normal so that the velocity distribution near the wall is isotropic in a hemisphere. These atoms enter the plasma where they are either ionized or undergo charge exchange collisions. The charge exchange collisions provide a first generation source for further generations of charge exchange by atoms born in the plasma. The velocity distribution of neutrals emerging from charge exchange events is isotropic and characteristic of the local ion temperature. Hence we distinguish between two populations of neutral atoms; those which came from the wall, which we call "cold," and those born in the plasma, which we call "hot."

On the basis of these assumptions, charge exchange events at the point  $\mathbf{r}$  constitute a source of energetic neutrals of energy  $\varepsilon$  described by

$$\phi(\mathbf{r}) g(\mathbf{r}, \varepsilon), \quad (1)$$

where

$$\int g(\mathbf{r}, \varepsilon) d\varepsilon = 1. \quad (2)$$

The function  $\phi(\mathbf{r})$  is the charge exchange source density at  $\mathbf{r}$  while  $g$  is the locally defined energy distribution of the emergent neutrals. Let there also be an external source of hot neutrals,  $\phi^0(\mathbf{r})$ , which are due to charge exchange by cold neutrals, recombination, etc. Then as is shown in Appendix A the neutral source density satisfies the integral equation

$$\phi(\mathbf{r}) = \phi^0(\mathbf{r}) + \int G(\mathbf{r}, \mathbf{r}') \phi(\mathbf{r}') d^3r', \quad (3)$$

where

$$G(\mathbf{r}, \mathbf{r}') = \int a^x(\mathbf{r}, \varepsilon) \frac{e^{-\tau(\mathbf{r}, \mathbf{r}', \varepsilon)}}{4\pi |\mathbf{r} - \mathbf{r}'|^2} g(\mathbf{r}', \varepsilon) d\varepsilon. \quad (4)$$

In Eq. (4)  $\tau$  is the optical depth

$$\tau(\mathbf{r}, \mathbf{r}', \varepsilon) = \int_{\mathbf{r}}^{\mathbf{r}'} \alpha^t(\mathbf{r}'', \varepsilon) dr'', \quad (5)$$

where the integral is taken along the path from  $\mathbf{r}'$ , to  $\mathbf{r}$ . The symbol  $\alpha(\mathbf{r}, \varepsilon)$  denotes the reciprocal mean free path at  $\mathbf{r}$  of a neutral atom of energy  $\varepsilon$ . Superscripts  $x, i, t$  denote charge exchange, ionization, and total, respectively. In each case  $\alpha$  is equal to the plasma density multiplied by a suitable average of the cross section over a thermal distribution.

To reduce (3) to a set of algebraic equations the cylindrical volume is divided into a number of coaxial zones in each of which the plasma properties are spatially uniform. Let the zone boundary radii be denoted by  $R_i$  and let the  $i$ th zone be bounded by  $R_i$  and  $R_{i-1}$ . We define  $\phi_i$  to be the average value of  $\phi$  in that zone:

$$\phi_i = \frac{1}{V_i} \int_{V_i} \phi(\mathbf{r}) d^3r, \quad (6)$$

where  $V_i$  is the zone volume in an annulus of unit height. If in the right-hand side of (3)  $\phi$  is approximated by its average value in each zone, then we obtain the set of algebraic equations

$$\phi_i = \phi_i^0 + \sum_j K_{ij} \phi_j, \quad (7)$$

where

$$K_{ij} = \frac{1}{V_i} \int_{V_i} d^3r \int_{V_j} d^3r' G(\mathbf{r}, \mathbf{r}') \quad (8)$$

The main task of the code, and by far the most time consuming, is the calculation of the matrix  $K$ . Once  $K$  is known the solution of Eq. (7) and construction of the output data are fast and straightforward.

Finally, the calculation of the kernel is enormously simplified if we assume  $g$  in each zone to be monoenergetic at the thermal energy corresponding to that zone, i.e.,

$$g(\mathbf{r}, \varepsilon) = \delta(\varepsilon - \varepsilon_r), \quad (9)$$

where  $\varepsilon_r$  is the thermal energy at  $\mathbf{r}$ . Equations (4) and (5) then become

$$G(\mathbf{r}, \mathbf{r}') = \alpha^x(\mathbf{r}, \mathbf{r}') \frac{e^{-\tau(\mathbf{r}, \mathbf{r}')}}{4\pi |\mathbf{r} - \mathbf{r}'|^2}, \quad (10)$$

$$\tau(\mathbf{r}, \mathbf{r}') = \int_{\mathbf{r}}^{\mathbf{r}'} \alpha^t(\mathbf{r}'', \mathbf{r}') dr'', \quad (11)$$

$$\varepsilon_r = \frac{3}{2} kT(\mathbf{r}). \quad (12)$$

The notation  $\alpha(\mathbf{r}, \mathbf{r}')$  is used to denote the absorption coefficient at  $\mathbf{r}$  for neutrals born at  $\mathbf{r}'$ . Notice that the  $G$  defined by Eq. 10 is not symmetric since the particle energy is tied to the temperature at  $\mathbf{r}'$ .

To completely specify a problem it is also necessary to know  $\phi_i^0$ , the inhomogeneous term in Eq. (7). The sources which are due to recombination or neutral beam capture must be provided externally. That part which is due to cold neutrals from the wall which penetrate to zone  $i$  is calculated by the code in much the same manner as  $K_{ij}$ .

At this point Eq. (7) describes a system with absorbing boundaries, i.e., atoms which leave the plasma are never returned. If an appreciable number of emerging fast neutrals are recycled at the wall they can significantly modify the net particle and energy transport. To the extent that the recycled atoms can be considered as belonging to the cold population this effect is trivial and easily accounted for outside of the transport code. In general, however, the recycled atoms will have a broad energy distribution ranging from essentially zero up to the incident energy, and proper inclusion of these neutrals is more complicated. There is a reasonably simple way in which this process can be included in the present code. To do this we take advantage of the property that a kind of group structure is provided by the fact that each zone has a unique thermal energy,  $\epsilon_i$ , associated with it. We can then classify the reflected particles according to the zone number with the same thermal energy, which establishes a one to one correspondence between energy group and zone numbers. To obtain a full description of recycling we first define the following quantities:  $W_i$  = probability that atoms born in zone  $i$  survive to reach the wall,  $R_{ji}$  = probability that an atom of energy  $i$  is recycled into energy group  $j$ ,  $\Gamma_{ij}$  = probability that atoms from wall in group  $i$  undergo charge exchange in zone  $j$ , and  $T_{ij} = t_i \delta_{ij}$  = probability that neutrals from the wall in group  $i$  traverse the entire plasma without interaction and return to the wall. In terms of these quantities it is easy to verify that the modification to  $K$  which includes the proper boundary condition is

$$K \rightarrow K + \Gamma(1 - RT)^{-1}RW. \quad (13)$$

This modification includes recycling in a fully implicit fashion and requires no iteration. The code presently calculates the quantities  $W$ ,  $T$ , and  $\Gamma$ . The matrix  $R$  contains all of the wall interaction physics which must be supplied by a suitable subroutine. Although we have been unable to find sufficient experimental or theoretical results for calculation of realistic reflection coefficients we have incorporated a simple reflection model which, while not physical, does include most of the required logic. In particular, we assume that the neutrals arriving at the wall are diffusely reflected with no energy change and that the reflection coefficient is independent of energy. The reflection is supplied as input data and if it is non-vanishing the  $\Gamma$  matrix is calculated as described below. It will be easy to include a more realistic model when the required data are available. As it is presently implemented the recycling option increases the running time by almost a factor of 2.

## 3. METHOD OF COMPUTATION

In Appendix B it is shown how calculation of the elements of  $K$  is reduced to a single quadrature. The integration variable,  $y$ , is essentially the distance of closest approach to the axis of a family of trajectories lying in the plane  $z = 0$ . For each value of  $y$  Eq. (B10) expresses the contribution of that ray to  $K_{ij}$  for all pairs of zones crossed by that trajectory. In practice, of course, the integration is replaced by a discrete sum. The most direct way of evaluating  $K$  would be to choose an  $i, j$  pair, perform the numerical integration with respect to  $y$  and proceed to another zone pair. However, the tracking along a given ray generates geometrical data for that ray which can be used in the computation for other zone pairs, and it is clearly more efficient to use a scheme where all the tracking data computed for a given  $y$  are used before proceeding to the next  $y$ . We therefore use an integration scheme which, in effect, calculates all elements of  $K$  simultaneously. The essentials of the scheme are as follows: Consider a fixed value of  $y$  and its corresponding ray, and let  $j$  represent the left most segment of that ray. Starting at  $j$  we march to the right and as each zone is crossed calculate the appropriate term in the integral of (B10) which gives the contribution of that ray to the corresponding  $K_{ij}$ . When the right hand boundary is reached we calculate  $W_j$ . By appropriate bookkeeping the contribution to  $T$  and to the  $F$  matrix are also obtained, and when the last zone is crossed  $j$  is moved one zone to the right and the process repeated until  $j$  reaches the right end. At this point the code proceeds the next  $y$  value and starts over.

It remains to choose a quadrature scheme for the  $y$  integration. A simple method for which the weights are independent of  $i, j$  is the following. The  $y$  axis is divided into  $N$  intervals by the zone radii  $R_n$ . In each interval choose a value of  $y_n$  at which the integrand in (B10) is evaluated. If the width of the  $n$ th zone =  $\delta_n$  then we approximate

$$\int_0^R f(y) dy \quad \text{by} \quad \sum_{n=1}^N f(y_n) \delta_n.$$

The choice of values for  $y_n$  is still not determined, and we choose them in such a way as to guarantee particle and energy conservation. It is obvious that each path integration is identically conservative, but the final  $K$  matrix is in general not. Consider the  $n$ th ray and its intersection with the  $i$ th. zone, defining a segment of length  $l_{in}$ . To each segment we associate a rectangle of width  $\delta_n$  which is shown as the shaded area in Fig. 1. It is easy to show that if the sum of the shaded areas in each zone equals the cross sectional area of the zone, i.e.,

$$V_i = \sum_n l_{in} \delta_n,$$

then  $K$  is identically conservative. This scheme requires tracking exactly  $N$  rays. Better accuracy is obtainable by further subdividing the  $y$  interval but we have learned from numerous examples that the gain in accuracy is typically a few percent which is not significant in view of our other approximations.

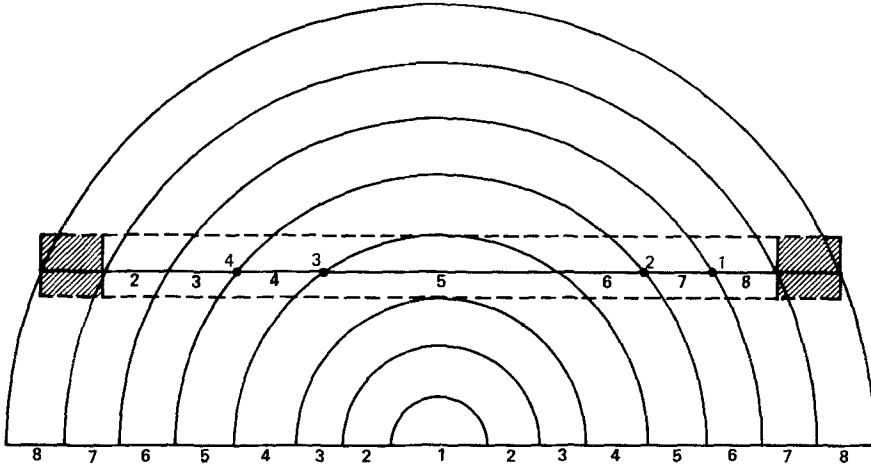


FIG. 1. Trajectory through the mesh of a typical ray. Intersections of ray with boundaries of zones  $i=6$ ,  $j=5$  are numbered. Dotted lines indicate boundaries of swath represented by the ray. Shaded areas indicate volume defined by the intersection of the swath with zone 8 as approximated in the code. Values of the index labelling the zone crossings are indicated along the ray. Zone numbers are along the  $x$  axis.

The most important outputs from the code are the rates of change of plasma particle density and energy due to neutrals. They are easily obtained once  $\phi$  is known. In particular the net rate of creation of plasma ions from hot neutrals in the  $i$ th zone is

$$\dot{\rho}_i = \sum_j \frac{\alpha_{ij}^i}{\alpha_{ij}^x} K_{ij} \phi_j. \quad (14)$$

Similarly the energy deposited in a zone by hot neutrals is

$$\dot{Q}_i = \sum_j \left[ \varepsilon_i \frac{\alpha_{ij}^i}{\alpha_{ij}^x} - \varepsilon_j \right] K_{ij} \phi_j. \quad (15)$$

Corresponding expressions for the contribution of the cold neutrals are

$$\dot{\rho}_i = \frac{\alpha_i^i}{\alpha_i^x} \phi_i^0 \quad \text{and} \quad \dot{Q}_i = \left[ \varepsilon_0 \frac{\alpha_i^i}{\alpha_i^x} - \varepsilon_i \right] \phi_i^0, \quad (16)$$

where  $\alpha_i$  is the absorption coefficient in zone  $i$  for the cold group and  $\varepsilon_0$  is the energy of the cold group. The contribution of the energy required to ionize is small and has been neglected. For the purpose of comparison with other codes we also compute the neutral density in each zone given by

$$n_i = \sum_j \frac{K_{ij} \phi_j}{v_j \alpha_{ij}^x} \quad (17)$$

for the hot neutrals and

$$n_i^0 = \frac{\phi_i^0}{v^0 \alpha_i^x} \quad (18)$$

for the cold group. Finally the code also provides the total current to the wall of neutrals from each zone which is in effect a crude spectrum of the emergent particles.

A major fraction of the running time is spent in evaluating  $H_3$  functions, since the number to be calculated scales as  $N^3$ . To speed this up we express the function as  $\exp(-\tau)$  times a slowly varying function which is approximated by a polynomial. Running time on the CDC 7600 for a 20 zone problem is typically  $\sim 0.12$  seconds. A version of the code exists which calculates the  $H_3$  function by look up and interpolation in a table which is generated only once. This version is somewhat faster at the expense of additional storage requirements. For a modest number of zones this code appears to be appreciably faster than other comparable codes for which we have information. Obviously, however, for a very large number of zones, the  $N^3$  scaling makes this scheme less attractive. The crossover at which, for example, the Hughes and Post code becomes faster is in the neighborhood of 40 zones.

#### 4. NUMERICAL RESULTS

The charge exchange cross section used by the code is taken from [6]. For neutrals of energy  $\varepsilon$  in a zone of ion temperature  $T_i$  (eV) we define

$$\varepsilon_+ = (\varepsilon + 4T_i/\pi)/A, \quad w = (A\varepsilon_-/\varepsilon)^{1/2}, \quad (19)$$

where  $A$  is the atomic number, and

$$\bar{\sigma}_x = 6.94 \cdot 10^{-15} w \times (1 - 0.155 \log_{10} \varepsilon_+)^2 / (1 + 1.12 \cdot 10^{-15} \varepsilon_+^{3.5}). \quad (20)$$

The rate for ionization by electron impact is adapted from (7) and given by

$$v^{-1} \bar{\sigma}_v = 7.25 \cdot 10^{-7} \times 10^{-(0.515 \log_{10} T_e) - 2.563/\log_{10} T_e - 5.231} (A/\varepsilon)^{1/2} \quad (21)$$

for  $T_e > 2$  eV and zero otherwise. For ionization by ion impact we use a simple fit to the curves in [8] which is valid for  $10^3 \lesssim T_i \lesssim 4 \times 10^4$ ,

$$v^{-1} \bar{\sigma}_v = 1.51 \cdot 10^{-16} w \cdot 10^{-1.15(4.4 - \log_{10} \varepsilon_+)^2}. \quad (22)$$

Figure 2 displays results of a test problem comparing the total neutral density and mean energy as computed by ANTIC and given by Hughes and Post [6] for a small low temperature plasma. Differences between these results are insignificant particularly in view of the simplified cross sections used. Results of a similar comparison with computations by Burrell [4] are not shown since the results are indistinguishable on the scale to which the graphs can be read. To test the code at higher temperature we have run the cases for the TFTR regime described by Gilligan



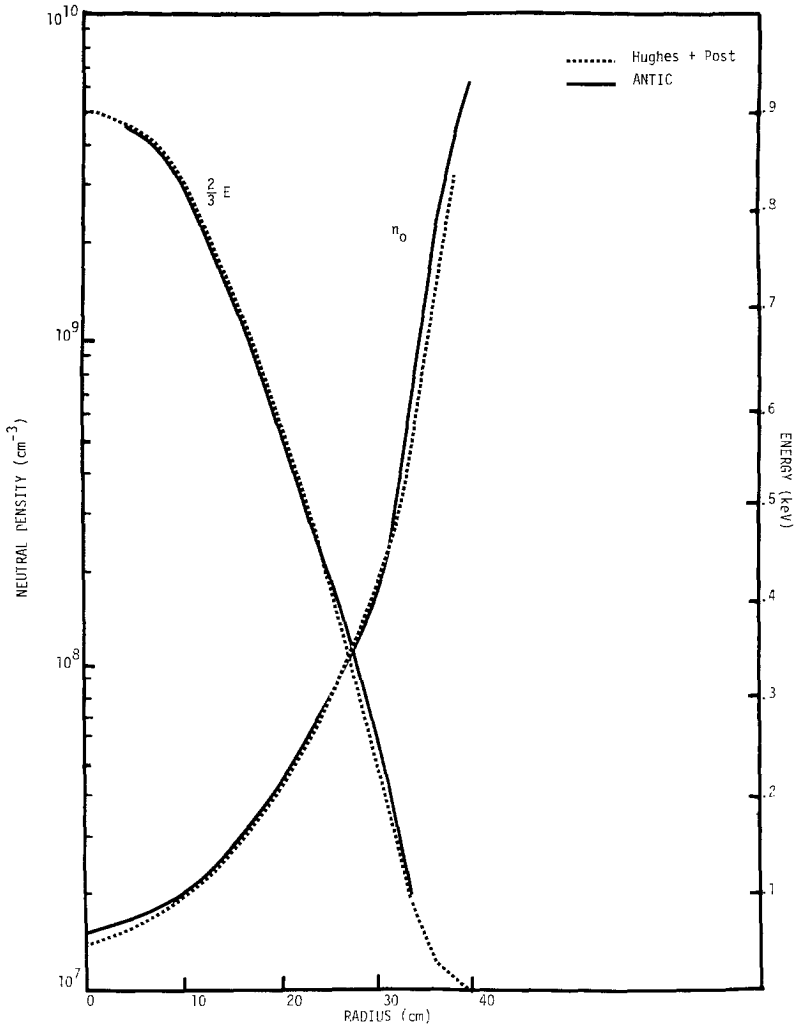


FIG. 2. Comparison of ANTIC calculation and results of [6]. Neutral density and "temperature" are plotted as functions of radius. Plasma parameters are  $n_e = n_i = 5 \times 10^{13} [1 - (r/a)^2] \text{ cm}^{-3}$ ,  $T_e = 2 \times 10^3 [1 - (r/a)^2] \text{ eV}$ ,  $T_i = 1 \times 10^3 [1 - (r/a)^2] \text{ eV}$ . The plasma radius,  $a$ , is 40 cm and the cold neutrals enter with 3 eV and carry a flux =  $5.98 \times 10^{15} \text{ cm}^{-2} \text{ sec}^{-1}$  corresponding to an edge density of  $10^{10} \text{ cm}^{-3}$ .

*et al.* [2]. The density profiles in Fig. 3 agree very well but with a minor discrepancy in the inner zones. It is not clear whether this difference is due to the breakdown of the isotropic scattering assumption at high energies, or to the very crude expression we use for the ion impact ionization cross section.

While calculation of neutral density profiles are in excellent agreement with other codes, one expects that the neutral energy distribution will be less accurate in view of our replacement of the thermal distribution in each zone by a monoenergetic spectrum. To test this we have attempted to compare the ANTIC calculation of the

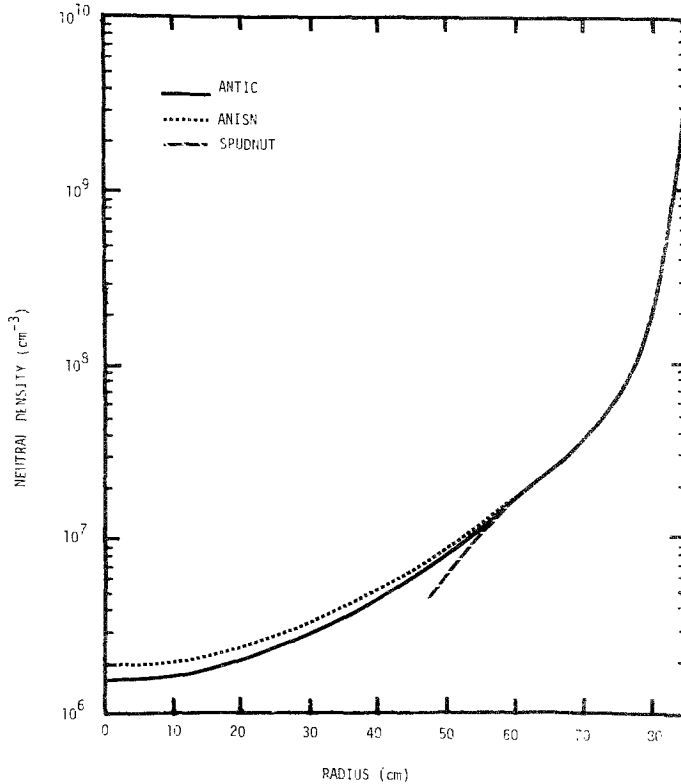


FIG. 3. Comparisons of neutral density profiles computed by ANTIC, from ANISN [2] and from SPUDNUT [5] for a TFTR plasma. Plasma profiles are  $n_e = n_i = [4(1 - (r/a)^2) + 1] \times 10^{13} \text{ cm}^{-3}$ ,  $T_e = T_i [9.95(1 - (r/a)^2) + 0.05] \text{ keV}$ . The plasma radius,  $a$ , is 85 cm and the cold neutral in flux is the same as in Fig. 2.

spectrum of neutrals emerging from the plasma with the results of [2]. This is done by taking the code output of the emergent flux of neutrals born in each zone and converting it into an energy spectrum by associating with each zone a corresponding energy bin of width given by the density of zone temperatures. The resulting comparison is shown in Fig. 4. The major difference between the two spectra is due simply to the loss of the high energy tails in our model. At the low end of the spectrum ANTIC gives a minimum energy corresponding to the temperature of the coldest zone, which depends strongly upon the fineness of the zoning near the plasma edge. However, in the interval between  $3/2$  times the lowest and highest zone temperatures the agreement is surprisingly good. Since the part of the spectrum carrying the great bulk of the energy is well represented, this spectrum should be good enough to use as input for a meaningful wall recycling calculation.<sup>1</sup>

<sup>1</sup> It was pointed out by one of the referees that a better calculation for the spectrum is needed for the interpretation of neutral spectra. This can easily be done, just as in [5], and we intend to add this feature in the near future.

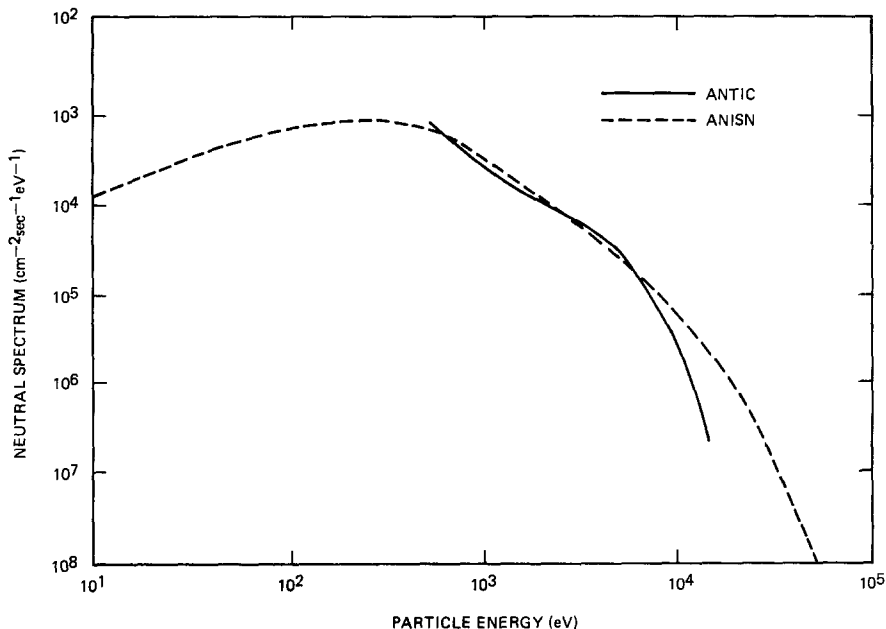


FIG. 4. Comparison of energy spectra of emergent neutral for the same case as Fig. 3.

### SUMMARY

We have described a code which solves the transport problem for neutral atoms in a cylindrical plasma by solution of the integral equation for the local neutral source density. The basic simplifying assumption which makes the scheme feasible is that charge exchange events in a given zone create an isotropic distribution of monoenergetic neutrals with energy equal to  $3/2$  times the local ion temperature. Comparison with other codes gives excellent agreement even at temperatures up to 10 keV.

### APPENDIX A: DERIVATION OF THE INTEGRAL EQUATION

We here derive the basic integral equation for the source density  $\phi(\mathbf{r})$ . Let the number of neutral atoms of energy  $\epsilon$  created per unit volume per unit time in the vicinity of  $\mathbf{r}$  be  $\phi(\mathbf{r})g(\mathbf{r}, \epsilon)$ , where  $g$  is the normalized energy distribution function and  $\phi$  is the total source strength. The source is the sum of two contributions; an external source,  $\phi^0$ , (such as recombination) and charge exchange events due to neutrals born elsewhere in the plasma. Let the neutrals be described in terms of a distribution

function  $f(\mathbf{r}, \boldsymbol{\Omega}, \varepsilon)$  where  $\varepsilon$  is the energy and  $\boldsymbol{\Omega}$  the direction of flight. In terms of  $f$  the source density can be written

$$\phi(\mathbf{r}) = \phi^0(\mathbf{r}) + \int v(\varepsilon) \alpha^x(\mathbf{r}, \varepsilon) f(\mathbf{r}, \boldsymbol{\Omega}, \varepsilon) d\boldsymbol{\Omega} d\varepsilon, \quad (\text{A1})$$

where  $\phi^0$  is the external contribution,  $v$  the speed corresponding to  $\varepsilon$ , and  $\alpha^x$  the reciprocal mean free path for charge exchange of an atom of energy  $\varepsilon$ .  $\alpha$  can be written as the local plasma density times a suitably averaged charge exchange cross section. We can also define a reciprocal mean free path for ionization,  $\alpha^i$  and a total  $\alpha^t = \alpha^x + \alpha^i$ .

The distribution function satisfies a Boltzmann equation

$$\boldsymbol{\Omega} \cdot \nabla f(\mathbf{r}, \boldsymbol{\Omega}, \varepsilon) + \alpha^t(v, \varepsilon) f(\mathbf{r}, \boldsymbol{\Omega}, \varepsilon) = \frac{\phi(\mathbf{r}) g(\mathbf{r}, \varepsilon)}{4\pi v(\varepsilon)}. \quad (\text{A2})$$

For fixed  $\boldsymbol{\Omega}$  we can choose a coordinate system with  $z$  axis parallel to  $\boldsymbol{\Omega}$  so  $\boldsymbol{\Omega} \cdot \nabla$  becomes  $\partial/\partial z$ , and for every  $x, y$  the solution of (A2) is

$$f(z, \varepsilon) = f(z_0, \varepsilon) = \int_{z_0}^z e^{-\int_{z_0}^z \alpha^t(z'', \varepsilon) dz''} \frac{\phi(z) g(z, \varepsilon)}{4\pi v(\varepsilon)} dz \quad (\text{A3})$$

for any  $z_0 < z$ . Writing  $z' - z = s$  and assuming no external sources (A3) is equivalent to

$$f(\mathbf{r}, \boldsymbol{\Omega}, \varepsilon) = \int_0^\infty e^{-\int_0^s \alpha^t(\mathbf{r} - \boldsymbol{\Omega}s', \varepsilon) ds'} \frac{\phi(\mathbf{r} - \boldsymbol{\Omega}s) g(\mathbf{r} - \boldsymbol{\Omega}s, s)}{4\pi v(\varepsilon)} ds. \quad (\text{A4})$$

We now insert the result into (A1) giving

$$\phi(\mathbf{r}) = \phi^0(\mathbf{r}) + \int \alpha^x(\mathbf{r}, \varepsilon) e^{-\int_0^s \alpha^t(\mathbf{r} - \boldsymbol{\Omega}s', \varepsilon) ds'} \frac{\phi(\mathbf{r} - \boldsymbol{\Omega}s) g(\mathbf{r} - \boldsymbol{\Omega}s)}{4\pi} ds d\boldsymbol{\Omega} d\varepsilon. \quad (\text{A5})$$

Finally multiplying numerator and denominator of the integrand by  $s^2$ , writing  $\mathbf{r}' = \mathbf{r} - \boldsymbol{\Omega}s$  and noting that  $s^2 ds d\boldsymbol{\Omega} = d^3 r'$  leads directly to the desired result, Eq. 4.

The physical meaning of Eqs. (4) and (A5) is simply that the charge exchange rate at  $\mathbf{r}$  is the neutral source strength at  $\mathbf{r}'$  multiplied by the probability that these atoms pass through a unit volume at  $\mathbf{r}$  times the probability of charge exchanging is that volume and integrated over all  $\mathbf{r}'$ , plus any externally produced sources.

## APPENDIX B: CALCULATION OF THE KERNEL $K_{ij}$

In this appendix we reduce the three-dimensional kernel obtained in Appendix A to one dimension and obtain its discrete approximation. The final result is an expression for each element of  $K$  in terms of a single integral.

We write Eqs. (3) and (10) in cylindrical coordinates and let the point  $\mathbf{r}$  lie in the plane  $z = 0$ . The integral is then

$$\phi(\mathbf{r}) = \phi^0(\mathbf{r}) + \int \alpha^x(\mathbf{r}, \mathbf{r} + \boldsymbol{\Omega}_\perp s) \phi(\mathbf{r} + \mathbf{r}_\perp s) \frac{e^{-\tau(\mathbf{r}, \boldsymbol{\Omega}_\perp, s)(1+z^2/s^2)^{1/2}}}{4\pi(z^2 + s^2)} s ds dz d\boldsymbol{\Omega}_\perp. \quad (\text{B1})$$

The point  $\mathbf{r}'$  is represented by its  $z$  coordinate and the projection of the ray from  $\mathbf{r}$  to  $\mathbf{r}'$  onto the plane  $z = 0$ . The latter is, in turn, described by its length,  $s$ , and the unit vector  $\boldsymbol{\Omega}_\perp$ . The optical thickness,  $\tau$ , is redefined to be measured along the projected path in the reference plane. Since all physical variables are independent of  $z$  this integration can be done at once. For this purpose and for subsequent calculations it is useful to introduce the set of functions

$$H_n(\tau) = \int_{-\infty}^{\infty} \frac{e^{-\tau(1+v^2)^{1/2}}}{(1+v^2)^{(n+1)/2}} dv = 2 \int_1^{\infty} \frac{e^{-\tau u}}{u^n(u-1)^{1/2}} du. \quad (\text{B2})$$

These functions satisfy

$$\begin{aligned} H'_{n+1}(\tau) &= -H_n(\tau), \\ H_0(\tau) &= 2K_0(\tau), \end{aligned} \quad (\text{B3})$$

where  $K_0$  is the usual modified Bessel function of the second kind. (Except for the factor 2 they are the  $Ki_n$  functions of [9].) Useful special values are

$$H_1(0) = \pi, \quad H_2(0) = 2, \quad H_3(0) = \pi/2, \quad (\text{B4})$$

while for  $\tau \gg 1$

$$H_n(\tau) \sim \left( \frac{2\pi}{\tau} \right)^{1/2} e^{-\tau}. \quad (\text{B5})$$

Equation (B1) then becomes

$$\phi(\mathbf{r}) = \phi^0(\mathbf{r}) + \frac{1}{4\pi} \int \alpha^x(\mathbf{r}, \mathbf{r} + \boldsymbol{\Omega}_\perp s) H_1(\tau) \phi(\mathbf{r}, \mathbf{r} + \boldsymbol{\Omega}_\perp s) ds d\boldsymbol{\Omega}_\perp. \quad (\text{B6})$$

To obtain  $\phi_i$  we average  $\phi(\mathbf{r})$  over the  $i$ th zone. Inverting the order of integration, axisymmetry implies that the integral is independent of  $\boldsymbol{\Omega}_\perp$  so there is no loss in generality in choosing it parallel to the  $x$  axis. The integrals are then evaluated by fixing  $y$  and carrying out the  $\mathbf{r}$  and  $\mathbf{r}'$  integration along  $y' = y$ ,  $x' < x$ .

The remaining steps require introduction of a certain amount of notation. Figure 1 represents the geometry of a typical track along  $y = \text{const}$  as it passes through the mesh. Numbers along the  $x$  axis are the numbers of the zones, while along the track we number the path segments from left to right by the index  $m$ . Note that there are in general two values of  $m$  for each zone. We define the symbol  $\sum_m^i$  to mean the sum

over all  $m$ 's crossing the zone  $i$ . For a typical pair of  $m$  values we label the points at which the ray crosses the zone boundaries from 1 to 4 as illustrated in the figure for  $i = 6, j = 5$ .

Since the  $\alpha$ 's are constant in each zone we can now write

$$\phi_i = \phi_i^0 + \sum_j K_{ij} \phi_j \tag{B7}$$

$$K_{ij} = \frac{\alpha_{ij}^x}{V_i'} \int_{-R_i}^{R_i} dy \sum_m^i \sum_{m'}^j \int_m \int_{m'} dx dx' H_1[\tau(x', x)]. \tag{B8}$$

The integrals along the path segments are now easily carried out using the recursion relations (B3). For given  $m$  and  $m'$ , a typical term in (B8) includes expressions of the form

$$\int_{x_2}^{x_1} dx \int_{x_4}^{x_3} dx' H_1[\tau(x', x)]. \tag{B9}$$

We consider separately the cases  $m \neq m'$  and  $m = m'$ .

*Case 1.  $m \neq m'$ .*

We note that  $dx' = -d\tau/\alpha'_{ij}$  and  $dx = d\tau/\alpha'_{ij}$  so that

$$\int_{x_4}^{x_3} dx' H_1[\tau(x', x)] = \frac{1}{\alpha'_{ij}} \{H_2[\tau(x_3, x)] - H_2[\tau(x_4, x)]\}.$$

Applying the same device to the  $x$  integration we obtain

$$\frac{1}{\alpha'_{ij} \alpha'_{jj}} \{H_3(\tau_{41}) - H_3(\tau_{31}) - H_3(\tau_{42}) + H_3(\tau_{32})\},$$

where  $\tau_{32} = \tau(x_3, x_2)$ , etc.

*Case 2.  $m = m'$ .*

For this case we need

$$\int_{x_2}^{x_1} dx \int_{x_2}^x dx' H_1[\tau(x', x)]$$

Using the same method this becomes

$$\frac{1}{\alpha'_{jj}} \int_{x_2}^{x_1} dx \{H_2(0) - H_2[\tau(x_2, x)]\} = \frac{1}{(\alpha'_{jj})^2} \{\tau_{12} H_2(0) - H_3(0) + H_3(\tau_{21})\}.$$

Combining these results we have

$$K_{ij} = \frac{2\alpha_{ij}^x}{V' \alpha_{ij}^t \alpha_{ij}^t} \int_0^{R_i} dy \sum_m^i \sum_{m'}^j I_{mm'} \quad (\text{B10})$$

$$\begin{aligned} I_{mm'} &= H_3(\tau_{41}) - H_3(\tau_{31}) - H_3(\tau_{42}) - H_3(\tau_{32}), & m \neq m' \\ &= 2\tau_{21} - H_3(0) + H_3(\tau_{21}), & m = m' \end{aligned} \quad (\text{B11})$$

Equations (B10) and (B11) provide the final expressions for the kernel which are actually evaluated by the code. The scheme for carrying this out is described in Section 3.

To specify the problem completely we also need expressions for  $W_i$ ,  $T_i$ , and  $\Gamma_{ij}$ . These are all calculated by the same method as above. In the code we assume atoms leave the wall with a cosine distribution, i.e., their angular distribution is isotropic in a hemisphere. It is easy to show that

$$\Gamma_{ij} = \frac{4}{V_i} \frac{\alpha_{ij}^x}{\alpha_{ij}^t} \sum_m^i \int_0^{R_i} [H_3(\tau_{32}) - H_3(\tau_{31})] dy, \quad (\text{B12})$$

where the point 3 is on the wall and point 1 and 2 are the end points of the path segment in zone  $i$ . Calculation of wall contribution to the inhomogeneous term,  $\phi_i^0$  is the same as that for  $\Gamma_{ij}$  but with  $\varepsilon_j$  replaced by the energy of the cold group.

Finally, the flux of atoms born in zone  $i$  which reach the wall per unit  $\phi_i$  is

$$W_i = \frac{1}{2\pi R \alpha_{ij}^t} \int_0^{R_i} [H_3(\tau_{23}) - H_3(\tau_{23})] dy \quad (\text{B13})$$

while the flux transmitted by the plasma per unit incoming flux is

$$T_i = \frac{2}{\pi R} \int H_3(\tau) dy, \quad (\text{B14})$$

where  $\tau$  is evaluated along the entire chord. It is in principle possible to allow the influx to be anisotropic. In this case the dependence upon polar angle will bring in  $H$  functions of order higher than 3 while the azimuthal dependence introduces an appropriate weight function in the  $y$  integration.

#### ACKNOWLEDGMENTS

The author wishes to thank Dr. James Gilligan for helpful discussion concerning his results and Ms. Laura Matteson for her assistance in construction of the polynomial approximation for the  $H_3$  function. This work was performed under auspices of the DOE Contract DE-ACO3-79ET53057.

## REFERENCES

1. E. GREENSPAN, *Nucl. Fusion* **14** (1974), 771.
2. J. G. GILLIGAN, S. L. GRALNICK, W. G. PRICE, JR. AND T. KAMMASH, *Nucl. Fusion* **18** (1978), 53.
3. J. T. HOGAN, "Methods of Computational Physics," (J. Killeen, Ed.), Vol. 16. Academic Press, New York, 1976.
4. K. H. BURRELL, *J. Comput. Phys.* **27** (1978), 88.
5. K. AUDENAERDE, G. A. EMMERT AND M. GORDINIER, *J. Comput. Phys.* **34** (1980), 268.
6. M. H. HUGHES AND D. E. POST, *J. Comput. Phys.* **28** (1978), 43.
7. D. F. DUCHS, D. E. POST AND P. M. RUTHERFORD, *Nucl. Fusion* **17** (1977), 565.
8. R. L. FREEMAN AND E. M. JONES, "Atomic Collision Processes in Plasma Physics Experiments." Culham Laboratory Report CLM-R 137.
9. M. ABRAMOWITZ AND I. A. STEGUN, "Handbook of Mathematical Functions," p. 483. National Bureau of Standards, Washington, D.C., 1962.